Catalysis Today 151 (2010) 223–230

Contents lists available at ScienceDirect

Catalysis Today

journal homepage: www.elsevier.com/locate/cattod

A comparative study of the NH_3-SCR reactions over a Cu-zeolite and a Fe-zeolite catalyst

Massimo Colombo, Isabella Nova, Enrico Tronconi [*]

Laboratory of Catalysis and Catalytic Processes, Dipartimento di Energia, Politecnico di Milano, Piazza Leonardo da Vinci 32, 20133 Milano, Italy

ARTICLE INFO

Article history:
Available online 9 February 2010

Keywords:
$DeNO_x$
Urea SCR
Cu-zeolite catalysts
Diesel exhausts aftertreatment

ABSTRACT

The NH_3-SCR (selective catalytic reduction) reactions were systematically investigated over a commercial copper zeolite catalyst in view of its application to the $DeNO_x$ aftertreatment of exhaust gases from light- and heavy-duty Diesel engines. Catalytic activity data were collected at high space velocities in both steady state and dynamic runs over the catalyst in the form of powder, in order to derive intrinsic kinetic information in a wide temperature range.

Results were also compared to those obtained over a commercial iron zeolite catalyst under similar conditions. With respect to the iron-based catalyst, the copper zeolite system showed a higher ammonia storage capacity, a higher activity in the ammonia oxidation reaction and in the Standard SCR reaction, and its $DeNO_x$ activity was found less sensitive to the NO_2 feed content. As opposite to the iron zeolite, over the copper zeolite no inhibiting effect of ammonia on the Standard SCR reaction was observed, while formation of some N_2O was detected even in the absence of NO_2 in the gas feed mixture.

1. Introduction

In order to reduce and control the emissions of NO_x from Diesel and other lean burn engines, the so-called primary techniques, which consist in limiting the formation of pollutants during the combustion process, are not sufficient. In this context the development of exhaust gas after-treatment technologies, i.e. technologies which are applied after the combustion process, plays a key role, especially in order to comply with the stricter and stricter Diesel emission standards that will become mandatory worldwide in the next few years (i.e. Euro 6 for Europe and Tier 2 for USA light duty vehicles).

The selective catalytic reduction of NO_x by ammonia/urea (NH_3/urea SCR technology), first developed for the abatement of NO_x from stationary sources [1], has been adapted in recent years to HD Diesel vehicles with excellent results [2].

Such a technology is based on the following main reactions:

$$4NH_3 + 4NO + O_2 \rightarrow 4N_2 + 6H_2O \qquad \text{Standard SCR} \qquad (1)$$

$$2NH_3 + NO + NO_2 \rightarrow 2N_2 + 3H_2O \qquad \text{Fast SCR} \qquad (2)$$

$$8NH_3 + 6NO_2 \rightarrow 7N_2 + 12H_2O \qquad NO_2\text{-SCR} \qquad (3)$$

The presence of NO_2 in the feed stream to the SCR converter is ensured by the installation of a Diesel Oxidation Catalyst (DOC) upstream of the SCR converter in the exhaust line. This is of critical importance in order to improve the SCR performances in the low temperature region, where the so-called ‘Fast SCR’ reaction (2) is by far more active [3–6] compared with the so-called Standard SCR reaction (1).

An enhanced catalytic activity is also essential to increase the overall $DeNO_x$ efficiency. In this context vanadium based catalysts have first been studied [7–10] because of their extensive industrial use in $DeNO_x$ processes for stationary applications. However, a number of reasons are now shifting the research interest towards other catalytic systems, including for example the need of higher activity at low temperatures, the need for catalysts active and stable up to higher temperatures, and the presence of carcinogenic vanadium in commercial V_2O_5–WO_3/TiO_2 catalysts [11].

Among the new emerging SCR catalytic systems for mobile applications, many efforts are focused on metal-promoted zeolites, which had been already proposed in the past for NO_x abatement in stationary installations as well [1,12–15]. Among such a wide family of catalysts, copper zeolites seem to be particularly interesting and have been extensively studied. Their catalytic behavior in NH_3-SCR of NO [16–20] and HC-SCR of NO_x [21–23] has been reported in the literature. More specifically, a few papers have also addressed the effect of the NO_2/NO_x feed ratio on the NH_3-SCR $DeNO_x$ activity over Cu-zeolites [4,24–26]. Nevertheless, in all of these works the catalyst was tested in the form of a washcoated honeycomb monolith, and relatively low space velocities, similar to those typical of real automotive applications, were always used.

The present work is devoted to the study of a state-of-the-art commercial copper-exchanged zeolite catalyst for NH_3-SCR

---

[*] Corresponding author. Tel.: +39 02 2399 3264; fax: +39 02 2399 3318.
E-mail address: enrico.tronconi@polimi.it (E. Tronconi).

0920-5861/$ – see front matter © 2010 Elsevier B.V. All rights reserved.
doi:10.1016/j.cattod.2010.01.010

applications to HD and LD Diesel vehicles. Specifically, the activity of this catalyst in all the main reactions typical of the NO–NO_2/NH_3-SCR reacting systems was investigated, and the results were compared with those obtained over a commercial iron-exchanged zeolite catalyst.

Notably, the two catalysts were tested in the form of powder, and many of the experiments herein reported were performed at space velocities much higher than those typical of automotive applications (up to 143,000 h^{-1}). With the catalyst in the powdered form, information about the prevailing network of reactions and their intrinsic kinetics can be obtained, which represents the first step in the development of an unsteady, chemically consistent mathematical model of real-scale urea SCR catalytic converters. Furthermore, working at high space velocities is of critical importance in order to emphasize kinetic effects over a wide range of temperatures.

2. Experimental

The experimental work was performed over a commercial catalyst originally supplied in the form of a cordierite honeycomb monolith (400 cpsi) washcoated with a Cu-zeolite. For comparison purposes, we report also data over a commercial honeycomb monolith washcoated with a Fe-zeolite; more information about this catalyst can be found in [27].

Both the original monolith catalysts were crushed and sieved to 140–200 mesh to avoid mass transfer limitations during testing. A sample of catalyst powder (60 mg for the copper zeolite, 80 mg for the iron zeolite) diluted with 60 mg of quartz powder was loaded in a flow-microreactor consisting of a quartz tube (6 mm i.d.) placed in an electrical furnace. All the lines upstream and downstream the reactor were heated to 200 °C to prevent H_2O condensation and NH_4NO_3 deposition. The concentrations of gaseous species (NH_3, NO, NO_2, N_2O, N_2) in the outlet stream were continuously monitored by a quadrupole mass spectrometer (Balzer QMS 200) and a UV analyzer (ABB-LIMAS 11 HV) in parallel. The reaction temperature was monitored and controlled by a *K*-type thermocouple immersed in the catalyst bed. He, NH_3, NO, NO_2, and O_2 were dosed to the gaseous feed stream by means of mass flow controllers (Brooks Instruments), while water vapor was added via a saturator operated at controlled temperature. Helium was used as carrier gas to enable evaluation of N-balances at steady state.

Catalysts conditioning consisted in a temperature ramp of 5 °C/min from room temperature up to 600 °C in 10% O_2 (v/v) + 10% H_2O, followed by hold at 600 °C for 5 h.

Catalytic activity runs were performed in the 50–550 °C temperature range, with feed concentrations of 0–500 ppm NH_3 and 0–500 ppm NO_x, and NO_2/NO_x ratios between 0 and 1. Water (3–10%, v/v) and oxygen (2–8%, v/v) were always present in the gaseous feed stream.

Temperature programmed desorption (TPD) and temperature programmed reaction (TPR) experiments were performed with a heating rate of 5 or 15 °C/min, while the reaction dynamics were investigated also by transient response (TRM) runs (step feed of NO_x and NH_3) under isothermal conditions within the 100–250 °C *T*-range. The system was operated at atmospheric pressure with flow rates ranging from 71 up to 327 cm^3/min (STP), corresponding to gas hourly space velocities (GHSV) referred to the active phase between 194,000 and 890,000 $cm^3/(h\ g_{cat})$ (STP). The flow rates were selected in such a way as to operate at the same space velocity over both the Cu- and the Fe-catalyst, in order to afford a direct comparison of the activity data. Considering the washcoat load of the original monolith catalysts, the space velocities referred to the equivalent monolith volume were between 31,000 and 143,000 h^{-1}. A detailed description of the experimental equipment and procedures can be found in [7,8,28–30].

3. Results and discussion

3.1. NH_3–O_2 reacting system

Since the $DeNO_x$ activity of SCR converters is governed by the reactivity of ammonia adsorbed onto the catalyst surface [31], the adsorption–desorption behavior of this individual species was first studied. For this purpose, a two-stage run was performed, wherein first a step feed change (TRM) (0–1000 ppm) of NH_3 at constant temperature (namely 200 °C) while flowing oxygen (2%), water (3%) and balance helium was performed, followed by a temperature programmed desorption (TPD) run.

Fig. 1A shows the reactor inlet and outlet ammonia concentration profiles during a TRM run performed over the copper zeolite catalyst at 200 °C: for the first 200 s after ammonia feed a “dead time” was observed in the ammonia outlet concentration profile. This transient is attributed to the adsorption of ammonia onto the catalyst since at 200 °C ammonia oxidation can be ruled out, as shown below. The approach to catalyst saturation resulted in the breakthrough of NH_3, its outlet concentration eventually reaching the feed value after about 1500 s.

The amount of adsorbed ammonia relative to the amount of catalytic active phase, i.e. the amount of washcoat powder, was estimated from the integral difference between the inlet and outlet

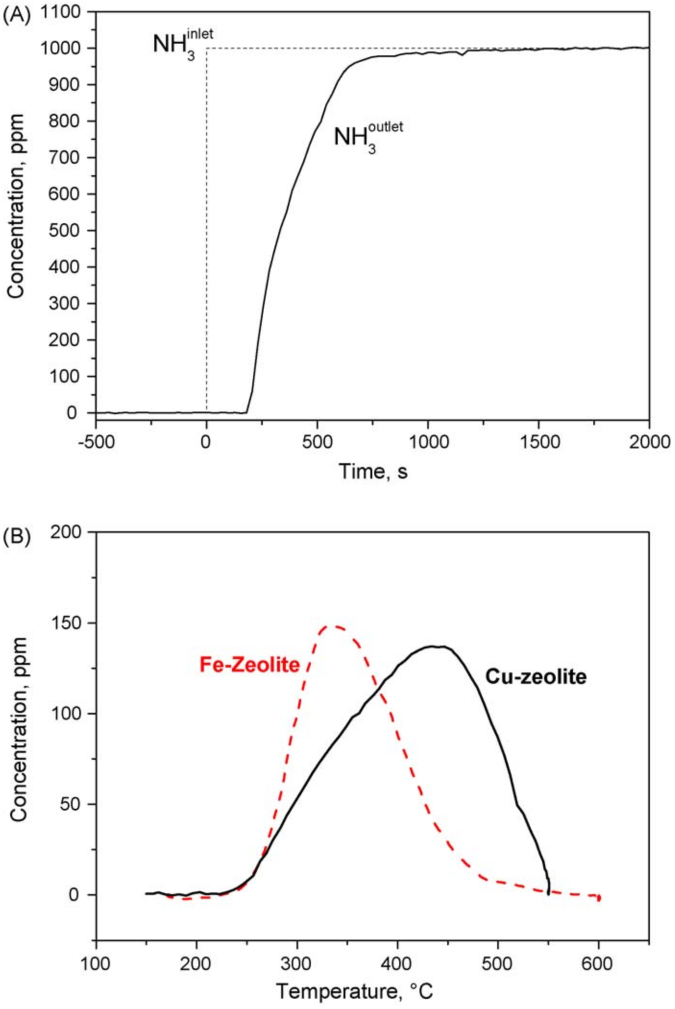

Fig. 1. (A) Ammonia adsorption on Cu-zeolite: *T* = 200 °C, *Q* = 71 cm^3/min (STP), NH_3 = 1000 ppm, H_2O = 3%, O_2 = 2%. (B) Ammonia TPD over Cu- and Fe-zeolite: *Q* = 71 cm^3/min (STP), H_2O = 3%, O_2 = 0%, *T* ramp = 15 K/min. Solid line = Cu-zeolite. Dashed line = Fe-zeolite.

NH_3 concentration profiles versus time, resulting in a storage capacity of about 1.3 mmol/$g_{active\ phase}$ at 200 °C.

After catalyst saturation, ammonia was removed from the feed flow, followed by oxygen removal, while the catalyst was continuously flushed with Helium and water for about 1.5 h. During this period of time a broad desorption tail (not reported in the figure) was observed, due to the desorption of weakly adsorbed ammonia.

In the final stage, the temperature was linearly incremented at 15 °C/min up to 550 °C. The solid line in Fig. 1B illustrates the ammonia outlet concentration profile as a function of catalyst temperature during the TPD run over the copper zeolite catalyst. As the temperature increased a broad desorption peak was observed, due to the release of the previously adsorbed ammonia. The amount of released ammonia relative to the amount of catalytic active phase was 0.36 mmol/$g_{active\ phase}$.

The dashed line in Fig. 1B shows the TPD results for the iron zeolite catalyst, which had been pretreated exactly as the Cu-zeolite sample. During the adsorption phase (not displayed in the figures) the storage capacity was about 0.60 mmol/$g_{active\ phase}$, thus significantly lower than on the copper zeolite. Furthermore, the amount of ammonia released during the TPD run was 0.177 mmol NH_3/$g_{active\ phase}$ in this case: it clearly appears that the tested iron zeolite catalyst was able to store a lower amount of strongly bonded ammonia as compared to the copper zeolite, too. The shape of the two TPD curves was also different. Indeed, the desorption of ammonia from the iron zeolite was essentially completed before reaching 500 °C, contrary to what observed for the copper zeolite, where NH_3 desorption was still significant at the same high temperature. Moreover, the maximum in the desorption peak was located at about 340 °C in the case of the iron zeolite, whereas it occurred at 440 °C for the copper zeolite. Such differences can be ascribed to the presence of NH_3 adsorption sites with different strengths on the two catalysts and/or to a different coverage dependence of the activation energy for ammonia desorption.

The ammonia oxidation reaction was then studied over both catalysts: experimental runs feeding 500 ppm of NH_3 in presence of oxygen (2%), water (3%) and balance helium at constant temperature were performed between 200 and 550 °C.

Fig. 2 shows the steady-state species outlet concentrations measured over the copper zeolite catalyst: ammonia started to be converted between 250 and 300 °C with production of nitrogen in agreement with the following stoichiometry

$$4NH_3 + 3O_2 \rightarrow 2N_2 + 6H_2O \qquad (4)$$

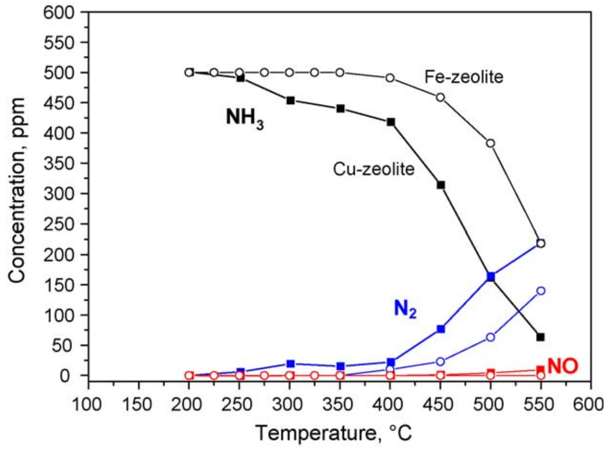

Fig. 2. Reactivity of NH_3–O_2 as a function of temperature over Cu- and Fe-zeolite: Cu-zeolite (full symbols): $Q = 245\ cm^3/min$ (890,000 $cm^3/h\ g_{active\ phase}$) (STP), NH_3 = 500 ppm, H_2O = 3%, O_2 = 2%. Fe-zeolite (open symbols): $Q = 327\ cm^3/min$ (890,000 $cm^3/h\ g_{active\ phase}$) (STP), NH_3 = 500 ppm, H_2O = 3%, O_2 = 2%.

At temperatures higher than 400 °C the ammonia conversion drastically increased, reaching about 90% at 550 °C. The data were consistent with the stoichiometry of reaction (4) up to 450–500 °C. Notably, 10 ppm of NO were detected at 550 °C. This could be a hint that ammonia is first oxidized to NO, which then readily reacts with ammonia according to (1). However, a more dedicated study, beyond the scope of the present work, would be needed to confirm such a two-step mechanism.

As also displayed in Fig. 2, the Fe-zeolite catalyst was less active in reaction (4). Indeed ammonia oxidation started to be significant only around 400 °C, reaching a maximum conversion of about 55% at 550 °C. No formation of NO was detected in this case.

3.2. NO–NO_2 reacting system

The adsorption–desorption behavior of NO onto the copper zeolite was first analyzed by means of TRM and TPD runs; experimental tests similar to those described for the NH_3–O_2 reacting system resulted in no evidence of significant NO storage onto the catalyst at 50, 100 and 175 °C, both in the presence and in the absence of oxygen.

The activity of the copper zeolite system in the reversible NO oxidation reaction (5),

$$2NO + O_2 \leftrightarrow 2NO_2 \qquad (5)$$

was then studied, since it is well known in the literature [4,6,32] that metal-promoted zeolite systems are active in such reactions.

For this purpose a temperature programmed reaction (TPR) experiment from 50 up to 550 °C was performed feeding 1000 ppm of NO in presence of oxygen (2%, v/v), water (3%, v/v) and balance

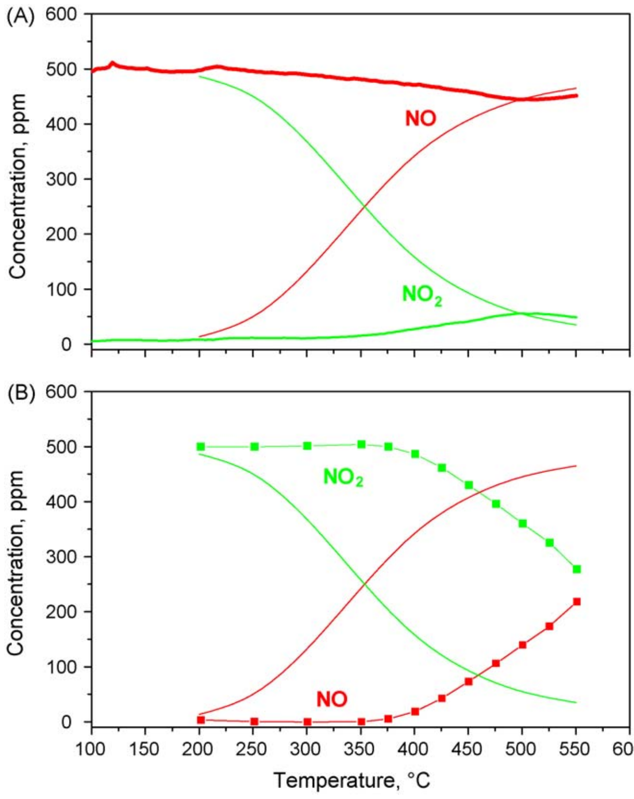

Fig. 3. (A) NO oxidation TPR run over Cu-zeolite: $Q = 71\ cm^3/min$ (258,000 $cm^3/h\ g_{active\ phase}$) (STP), NO = 500 ppm, H_2O = 3%, O_2 = 2%, T ramp = 5 K/min. (B) NO_2 decomposition over Cu-zeolite: $Q = 245\ cm^3/min$ (890,000 cm3/h $g_{active\ phase}$) (STP), NO_2 = 500 ppm, H_2O = 3%, O_2 = 2%. Thin lines = thermodynamic equilibrium values for NO and NO_2 concentrations.

helium: its results are compared with estimated chemical equilibrium concentrations in Fig. 3A. NO oxidation started above 200 °C reaching a maximum conversion of only 10% at about 500 °C in spite of the low space velocity. The outlet species concentrations were consistent with the stoichiometry of reaction (5). At higher temperatures (around 500 °C) thermodynamic equilibrium was approached, which explains the observed decrease of NO conversion as the temperature was further increased.

The reverse of NO oxidation, i.e. NO_2 decomposition, was also investigated by feeding 1000 ppm of NO_2 to the catalyst together with 2% (v/v) O_2, 3% (v/v) H_2O and balance helium. According to Fig. 3B NO_2 decomposition to NO started around 400 °C, reaching a maximum conversion of about 45% at 550 °C. The conversion was still far away from thermodynamic equilibrium under the adopted operating conditions.

The adsorption of NO_2 onto the copper zeolite catalyst was studied by feeding to the reactor 1000 ppm of NO_2 in the presence of oxygen (2%, v/v), water (3%, v/v) and balance helium at 200 °C. Fig. 4A shows that, after NO_2 was fed to the reactor at $t = 0$, two distinct features were observed: first the NO_2 outlet concentration trace showed a dead time, followed by a rapid increase approaching the feed concentration. The second observed process was an immediate NO evolution as NO_2 was fed to the reactor: the NO concentration reached a maximum value of about 300–330 ppm and then dropped back to zero following a mirror image of the NO_2 profile.

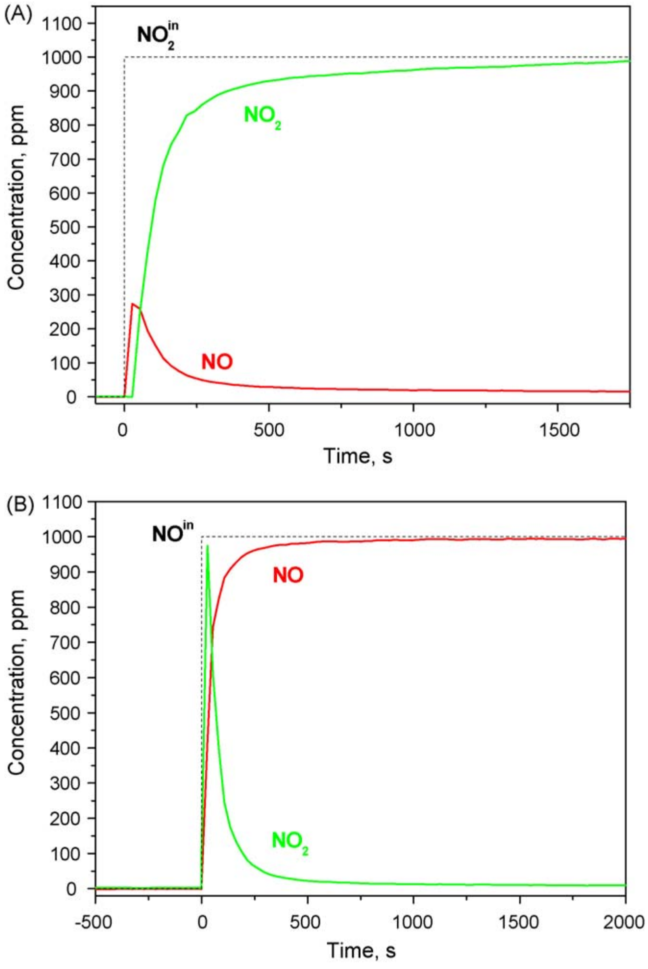

Fig. 4. (A) NO_2 adsorption on Cu-zeolite: $T = 200$ °C, $Q = 71\ cm^3/min$ (STP), $NO_2 = 1000$ ppm, $H_2O = 3\%$, $O_2 = 2\%$. (B) Reaction of nitrates with NO over Cu-zeolite: $T = 200$ °C, $Q = 71\ cm^3/min$ (STP), NO = 1000 ppm, $H_2O = 3\%$, $O_2 = 0\%$.

It has been reported in literature [6,30,33–38] that zeolite catalysts are able to adsorb NO_2 in the form of nitrates. The mechanism of NO_2 adsorption can be described by the following two-step sequence representing disproportion of NO_2 to form surface nitrites and nitrates, followed by NO_2 oxidizing the nitrites to nitrates:

$$2NO_2 + O^{2-} \leftrightarrow NO_3^- + NO_2^- \quad (6)$$

$$NO_2 + NO_2^- \leftrightarrow NO + NO_3^- \quad (7)$$

The combination of (6) and (7) results in the following global stoichiometry,

$$3NO_2 + O^{2-} \leftrightarrow NO + 2NO_3^- \quad (8)$$

where 1 mol of gaseous NO is produced for every three moles of adsorbed NO_2. In our experiments a $NO/\Delta NO_2$ ratio of about 0.35 was indeed observed over the copper zeolite system, in accord with the stoichiometry of (8). Accordingly such a mechanism of NO_2 adsorption could be reasonably acceptable also for the analyzed copper zeolite catalyst.

The amount of adsorbed nitrates relative to the amount of catalytic active phase, i.e. the amount of washcoat powder, was determined from Fig. 4A taking into account the stoichiometry of reaction (8), resulting in a storage capacity of about 0.4 $mmol/g_{active\ phase}$ at 200 °C.

To confirm the presence of nitrates onto the catalyst surface and to study their thermal stability, a TPD run was performed after saturation of the copper zeolite sample with NO_2 (results not shown). During the T-ramp evolution of NO_2, NO and oxygen were recorded, in line with what already observed for other zeolite systems [3,39].

The reactivity of the stored nitrates with NO was then investigated by means of a TRM run, whose results are presented in Fig. 4B: 1000 ppm of NO were fed to a catalyst whose surface had been pre-saturated with nitrates. The result was an initial conversion of NO with concurrent NO_2 formation (with a maximum peak concentration of about 1000 ppm). After a few seconds the NO signal reached the feed concentration value, while the NO_2 concentration rapidly decreased to zero. This behavior can be explained assuming reactions (6), (7), and thus reaction (8), to be reversible. Further information about the reactivity of NO with nitrates is presented in [27].

The same set of experiments for the analysis of the NO–NO_2 reacting system was performed also over the iron zeolite catalyst. Summarizing the main results, it can be said that no significant storage of NO was detected for this system, like for the copper zeolite. The tested iron zeolite was found also poorly active in the NO oxidation reaction, with a similar activity if compared to the copper zeolite. Furthermore tests for NO_2 adsorption and for the nitrates reaction with NO, which can be found in [27], showed the same qualitative behavior over both the copper and the iron zeolite systems, while quantitative differences were appreciable: e.g. the storage capacity of nitrates was greater over the Cu-zeolite.

3.3. NH_3–NO–NO_2–O_2 reacting system

3.3.1. Steady-state activity

The NH_3–NO–NO_2–O_2 SCR reactivity was then studied over the copper zeolite catalyst. The effect of the NO_2/NO_x feed ratio on the $DeNO_x$ activity was investigated, starting with the analysis of results obtained with no NO_2 in the feed stream ($NO_2/NO_x = 0$).

The SCR reactivity of the NO–NH_3–O_2 mixture was studied at steady-state conditions in the 150–550 °C temperature range. For this purpose 500 ppm of NO were continuously fed to the reactor

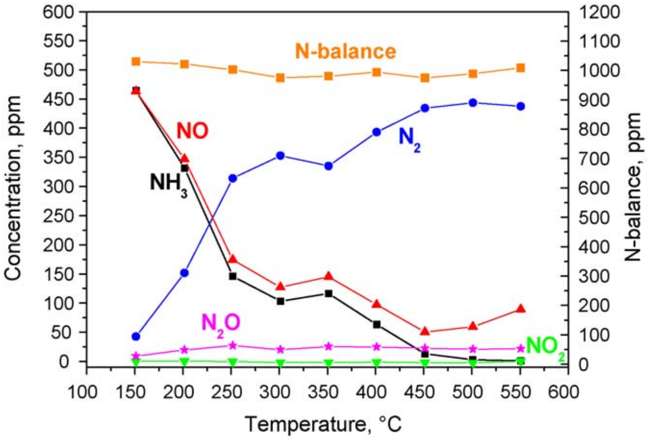

Fig. 5. Reactivity of NH_3–NO–O_2 as a function of temperature over Cu-zeolite: $Q = 245\ cm^3/min$ (890,000 $cm^3/h\ g_{active\ phase}$) (STP), NH_3 = 500 ppm, NO = 500 ppm, H_2O = 3%, O_2 = 2%.

together with 500 ppm of NH_3, O_2 (2%, v/v), H_2O (3%, v/v) and balance helium; the reactor temperature was kept constant until steady-state conditions were approached.

Fig. 5 illustrates the results of an experimental run over the copper zeolite catalyst in terms of NH_3, NO, NO_2, N_2 and N_2O outlet concentrations at steady state versus temperature. Reactants conversions, already significant at 150 °C, increased monotonically with temperature until 300 °C. At the lowest temperatures an equimolar consumption of NO and NH_3 was observed, but, on increasing the temperature, the NO/NH_3 molar consumption ratio shifted to values lower than unity. In the same temperature range an increasing evolution of nitrogen was detected. In the 150–300 °C *T*-range, outlet species concentrations were in line with the occurrence of the Standard SCR reaction (1): the slightly higher consumption of ammonia with respect to NO can be related to the onset of the ammonia oxidation reaction (4) already active in this temperature region [4,6,13,40].

At reaction temperatures between 300 and 350 °C, NO and NH_3 outlet concentrations showed a plateau. In the same *T*-range also the nitrogen production at steady state remained almost constant.

Upon further increasing the reaction temperature above 350 °C ammonia and NO outlet concentrations decreased, the NH_3 conversion reaching 100% at around 500 °C. Total conversion of NO was not reached because of the increasing importance of ammonia oxidation at high temperatures.

Evolution of N_2O (maximum value around 30 ppm) was also observed in the whole explored temperature range. The N-balance always closed within ±5% at steady state.

Additional experiments were run in the 150–550 °C temperature range with different O_2 (2–8%, v/v) and H_2O (3–10%, v/v) feed contents, in order to investigate their effects on the Standard SCR reaction. The results pointed out a promoting effect of oxygen (estimated reaction order around 0.45) and, on the contrary, a negligible effect of water concentration on the SCR activity.

The reactivity of NO_2 and ammonia over the copper zeolite system in the absence of NO ($NO_2/NO_x = 1$) was then addressed. Steady state results were collected in the 180–550 °C *T*-range feeding to the reactor 500 ppm of NH_3, 500 ppm of NO_2, O_2 (2%, v/v), water (3%, v/v) and balance helium.

According to Fig. 6, some catalytic activity was apparent already at 180 °C. Below 250 °C a 1/1 NO_2/NH_3 molar consumption ratio was observed, with a nitrogen production compatible with the stoichiometry of reaction (9) [3,8,9]

$$2NH_3 + 2NO_2 \rightarrow N_2 + NH_4NO_3 + H_2O \qquad (9)$$

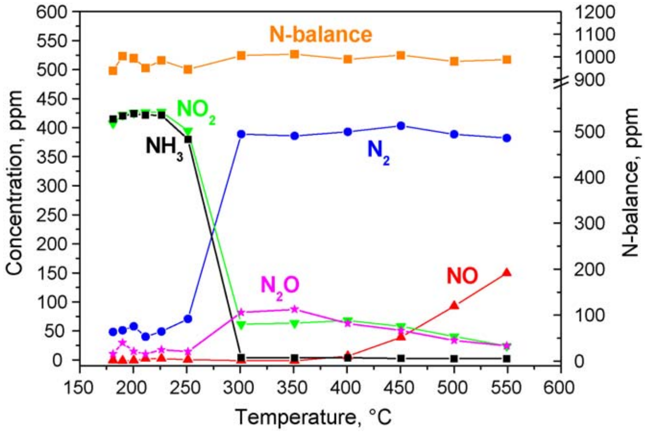

Fig. 6. Reactivity of NH_3–NO_2–O_2 as a function of temperature over Cu-zeolite: $Q = 245\ cm^3/min$ (890,000 $cm^3/h\ g_{active\ phase}$) (STP), NH_3 = 500 ppm, NO_2 = 500 ppm, H_2O = 3%, O_2 = 2%.

A lack in the N-balance was also apparent, again consistent with the formation of ammonium nitrate via reaction (9). Reactants conversions around 15%, scarcely dependent on temperature, were recorded in this T-window.

Above 250 °C the conversions of both reactants increased together with the nitrogen concentration. However the ammonia consumption was higher if compared to NO_2, reaching 100% conversion already at 300 °C. In this T-region the N-balance closed within ±5%. The sudden change of steady-state outlet concentrations could be ascribed to the light-off of the so-called NO_2-SCR reaction (3) [8,41,42], whose stoichiometry was well in accordance with the experimental data. Above 400 °C NO was also detected, likely the product of unreacted NO_2 which decomposed according to reaction (5) reverse.

Significant production of N_2O was observed above 250 °C with a maximum (about 90 ppm) at 300–350 °C. Its formation could be justified considering that the thermal decomposition of ammonium nitrate gives N_2O as a product, thus according to the following global reaction (10)

$$2NH_3 + 2NO_2 \rightarrow N_2O + N_2 + 3H_2O \qquad (10)$$

The study of the NO_2 effect on the DeNO$_x$ activity proceeded with the case of $NO_2/NO_x = 0.5$; these results were obtained feeding to the reactor 500 ppm of NH_3, 250 ppm of NO_2 and NO, O_2 (2%, v/v), H_2O (3%, v/v) and balance helium. Fig. 7 shows the species outlet concentrations measured at steady state in the 180–500 °C *T*-range.

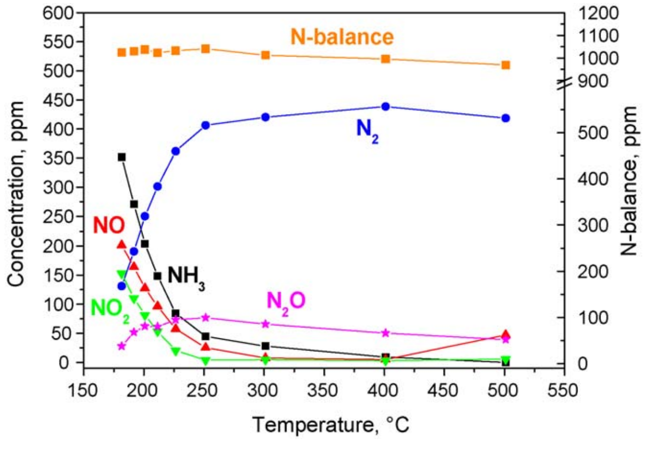

Fig. 7. Reactivity of NH_3–NO–NO_2–O_2 as a function of temperature over Cu-zeolite: $Q = 245\ cm^3/min$ (890,000 $cm^3/h\ g_{active\ phase}$) (STP), NH_3 = 500 ppm, NO = 250 ppm, NO_2 = 250 ppm, H_2O = 3%, O_2 = 2%.

At 180 °C a considerable $DeNO_x$ activity was already evident (30% conversion of both NO_x and ammonia); such an activity grew rapidly upon increasing the reaction temperature until 350–400 °C, where reactants conversion was almost complete. The nitrogen signal followed that of NO_x and ammonia as a mirror image until 400 °C; above this temperature the N_2 signal slightly decreased while NO was again detected. N_2O was also observed during the experimental run, with a maximum concentration of about 75 ppm around 250 °C, while the N-balance was more or less closed in the whole temperature range.

It is well known from the literature [3,4,6,24,43] that over zeolite catalysts in the presence of ammonia and of equimolar NO–NO_2 mixtures the so-called "Fast SCR" reaction (2) takes place. However it is worth emphasizing that below 300 °C we detected a difference in the conversions of NO and NO_2, which is at variance with the stoichiometry of reaction (2). This difference could be explained taking into account also reaction (10), that is the formation of nitrous oxide. N_2O was indeed observed in the whole investigated *T*-range: in fact its formation involves only the consumption of ammonia and NO_2, but not of NO.

Keeping a constant feed concentration of 500 ppm of total NO_x, steady-state activity data were also collected with intermediate NO_2/NO_x feed ratios of 0.25 and 0.75. In addition to NO_x, 500 ppm of NH_3, O_2 (2%, v/v), H_2O (3%, v/v) and balance helium were fed to the reactor in the 180–500 °C *T*-range, like in previous tests.

In Fig. 8A steady-state NO_x conversions over Cu-zeolite are plotted versus the NO_2/NO_x feed ratio, with temperature as a parameter. Thus, Fig. 8A provides a complete overview of the steady-state $DeNO_x$ activity over the analyzed Cu-zeolite catalyst for NO_2/NO_x ratios ranging from 0 to 1.

At all temperatures between 190 and 400 °C the maximum $DeNO_x$ activity was obtained with an equimolar feed ratio of NO and NO_2, while above 400 °C a decrease of NO_x removal efficiency was evident on increasing the NO_2 feed content, due to ammonia becoming the limiting reactant. Furthermore, it appears that in most of the temperature range NO_2/NO_x feed ratios ≤ 0.5 are preferable.

The NO_2/NO_x ratio effect was analyzed also in terms of N_2O production. Fig. 8B shows N_2O measured steady-state outlet concentrations versus temperature versus the NO_2/NO_x feed ratio. Notably, N_2O production was detected over the tested copper zeolite whether or not NO_2 was included in the feed stream; nevertheless higher concentrations were observed with NO_2/NO_x ratios ≥ 0.5. The nitrous oxide production was temperature dependent and its maximum value (around 90 ppm) was located between 250 and 350 °C, depending on the NO_2/NO_x feed content.

The reactivity of the NH_3–NO–NO_2–O_2 SCR reacting system was also investigated over the iron zeolite catalyst at different NO_2/NO_x feed ratios. In Fig. 9A the measured steady-state NO_x conversions at different temperatures are plotted versus the NO_2/NO_x feed ratio.

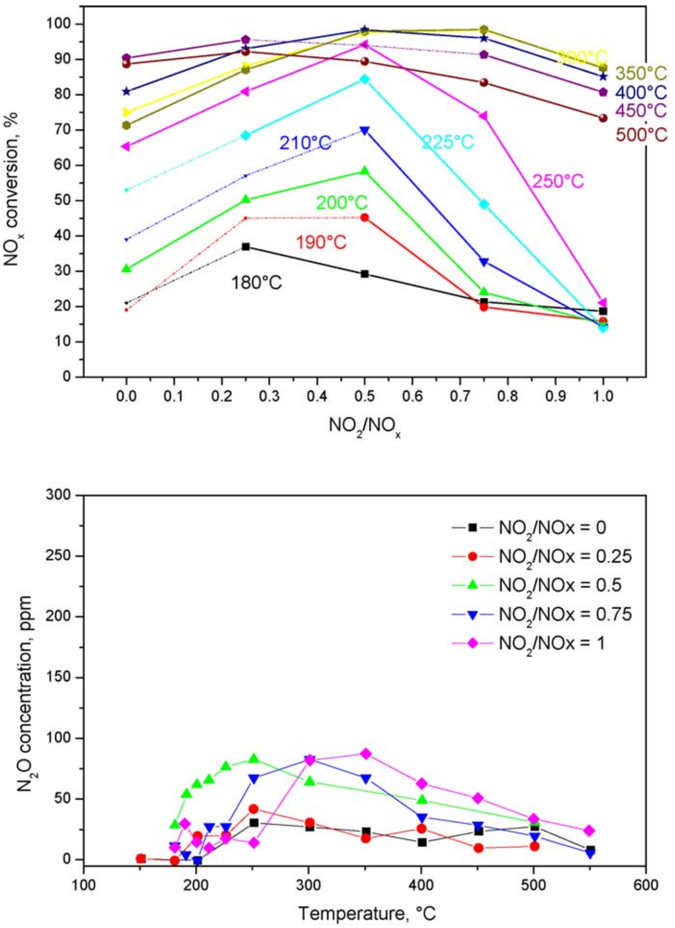

Fig. 8. (A) Effect of the NO_2/NO_x feed ratio on $DeNO_x$ activity over Cu-zeolite. $Q = 245\ cm^3/min$ ($890{,}000\ cm^3/h\ g_{active\ phase}$) (STP), $NH_3 = 500$ ppm, $NO_x = 500$ ppm, $H_2O = 3\%$, $O_2 = 2\%$, $T = 180$, 190, 200, 210, 225, 250, 300, 350, 400, 450 and 500 °C. (B) Effect of the NO_2/NO_x feed ratio on N_2O production over Cu-zeolite. $Q = 245\ cm^3/min$ ($890{,}000\ cm^3/h\ g_{active\ phase}$) (STP), $NH_3 = 500$ ppm, $NO_x = 500$ ppm, $H_2O = 3\%$, $O_2 = 2\%$.

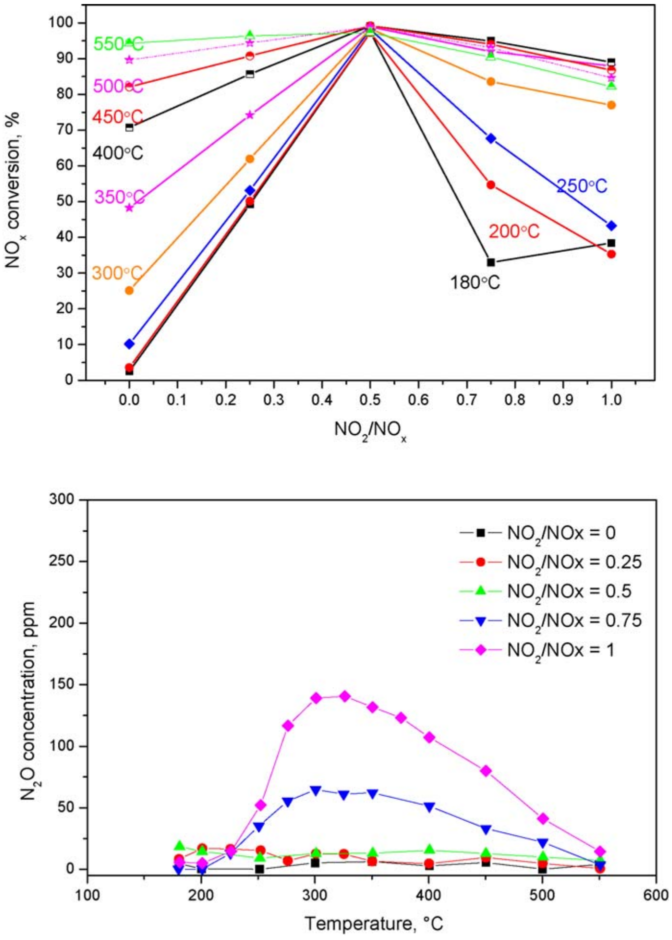

Fig. 9. (A) Effect of the NO_2/NO_x feed ratio on $DeNO_x$ activity over Fe-zeolite. $Q = 327\ cm^3/min$ ($890{,}000\ cm^3/h\ g_{active\ phase}$) (STP), $NH_3 = 500$ ppm, $NO_x = 500$ ppm, $H_2O = 3\%$, $O_2 = 2\%$, $T = 180$, 200, 250, 300, 350, 400, 450, 500 and 550 °C. (B) Effect of the NO_2/NO_x feed ratio on N_2O production over Fe-zeolite. $Q = 327\ cm^3/min$ ($890{,}000\ cm^3/h\ g_{active\ phase}$) (STP), $NH_3 = 500$ ppm, $NO_x = 500$ ppm, $H_2O = 3\%$, $O_2 = 2\%$.

Over this catalyst the $DeNO_x$ activity was more strongly dependent on the NO_2 feed content than over the copper zeolite system. Also, the iron zeolite exhibited a lower activity when low amounts of NO_2 were present in the feed stream. On the other hand, the light-off of the Fast SCR activity occurred at much lower temperature over the Fe-zeolite: as a result, at the optimal $NO_2/NO_x = 0.5$ feed ratio complete NO_x conversion was achieved already at 180 °C over the iron catalyst, but only at $T = 300$ °C over the copper zeolite.

Again for comparison purposes, Fig. 9B shows experimental results in terms of N_2O production over the iron zeolite catalyst. Steady-state N_2O outlet concentrations are plotted versus the NO_2/NO_x feed ratio in the 175–550 °C temperature region. Contrary to what observed with the copper zeolite system, significant N_2O production was detected only if an excess of NO_2 was present in the gas feed mixture, with a maximum value of about 150 ppm at 325 °C when NO_2 was the only source of NO_x ($NO_2/NO_x = 1$).

3.3.2. *Transient features*

Transient response runs in the presence of NO, NH_3 and O_2 were performed with the purpose of identifying the transient behavior of the copper zeolite catalyst, and comparing it to the behavior of the iron zeolite. In each isothermal run ammonia was fed to the reactor in a stepwise manner while continuously flowing NO (500 ppm with $NO/NH_3 = 1$), oxygen (2%, v/v), water (3%, v/v) and balance helium. When steady state was reached the ammonia feed was stopped and the run continued until a new steady-state condition was achieved. Such tests were performed at different temperatures between 100 and 250 °C.

Fig. 10 shows the evolution of the species outlet concentrations in a test performed at 175 °C over the copper zeolite catalyst. After feeding ammonia, the NO signal monotonically decreased approaching steady state, and the N_2 trace followed that of NO as a mirror image; meanwhile the ammonia signal, after a dead time, rose up approaching steady state. At ammonia shut-off, the nitrogen production gradually and monotonically decreased to zero as the NO concentration went back to its feed value, while the NH_3 signal quickly dropped to zero.

The same qualitative behavior was observed at 200 °C (Fig. 11A) and 250 °C, while at lower temperatures, namely 100 and 125 °C, minor transient features of the NO and N_2 concentration traces were observed upon ammonia start-up, but the steady-state SCR activity was practically absent.

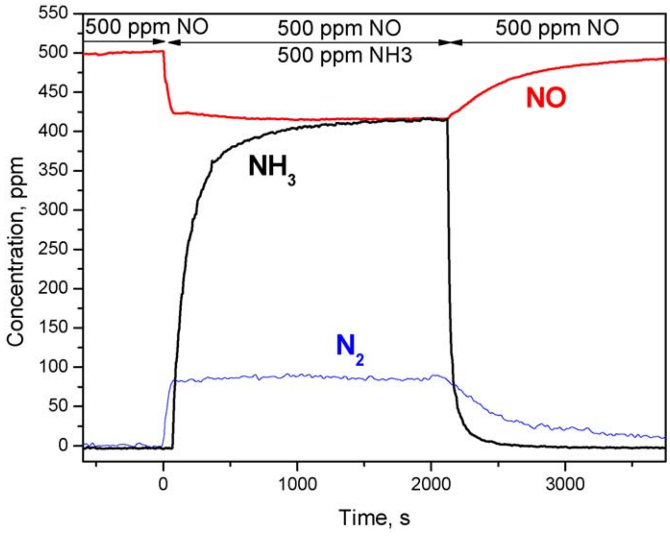

Fig. 10. Concentration step change experiment for the NH_3–NO–O_2 reacting system over Cu-zeolite: $T = 175$ °C, $Q = 245\ cm^3/min$ (890,000 $cm^3/h\ g_{active\ phase}$) (STP), $NH_3 = 500$ ppm, NO = 500 ppm, $H_2O = 3\%$, $O_2 = 2\%$.

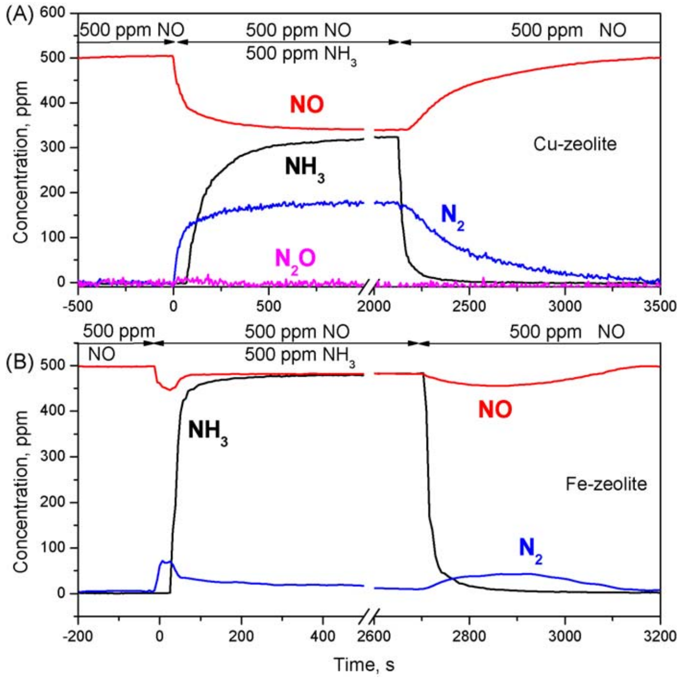

Fig. 11. (A) Concentration step change experiment for the NH_3–NO–O_2 reacting system over Cu-zeolite: $T = 200$ °C, $Q = 245\ cm^3/min$ (890,000 $cm^3/h\ g_{active\ phase}$) (STP), $NH_3 = 500$ ppm, NO = 500 ppm, $H_2O = 3\%$, $O_2 = 2\%$. (B) Concentration step change experiment for the NH_3–NO–O_2 reacting system over Fe-zeolite: $T = 200$ °C, $Q = 327\ cm^3/min$ (890,000 $cm^3/h\ g_{active\ phase}$) (STP), $NH_3 = 500$ ppm, NO = 500 ppm, $H_2O = 3\%$, $O_2 = 2\%$.

For comparison purposes, Fig. 11B illustrates the outlet species concentration profiles during a concentration step change test performed at 200 °C over the iron zeolite catalysts. In this case a maximum in the $DeNO_x$ activity was observed at both start-up and shut-off of the ammonia feed. Such transient features, already observed over different zeolite systems [44–46] as well as over V_2O_5–WO_3/TiO_2 SCR catalysts [31], have been explained invoking an inhibiting effect of ammonia [31], which clearly seems not to be significant for the analyzed copper zeolite catalyst, at least under the investigated experimental conditions.

4. Conclusions

The activity of a commercial copper-exchanged zeolite SCR catalyst for HD and LD vehicle applications has been systematically investigated in all the NH_3–NO–NO_2-SCR reactions by both steady state and transient experiments. The catalyst was able to adsorb ammonia and was active in its oxidation; NO_2 was also adsorbed on the catalyst surface in the form of nitrates, and the catalyst was active both in NO oxidation and in NO_2 decomposition as well. Furthermore the $DeNO_x$ activity of the catalyst and the N_2O production in NH_3-SCR reactions have been addressed as a function of the NO_2/NO_x feed ratio. The best $DeNO_x$ performances could be obtained always with NO_2/NO_x ratios close to 0.5, while some N_2O production was observed at all values of NO_2/NO_x, i.e. also in the absence of NO_2 in the feed stream. A peculiar behavior was noted in the case of the NH_3–NO–O_2 reacting system: when analyzing the reactants conversion as a function of temperature, a plateau was observed in the 300–350 °C *T*-range.

The results for the Cu-zeolite catalyst have been also compared with SCR data obtained over a commercial Fe-exchanged zeolite catalyst. The two catalytic systems exhibited similar qualitative behaviors, but important differences were apparent from a quantitative point of view. Specifically, the copper zeolite catalyst was associated with greater storage capacities of ammonia and nitrates, and with a greater activity in the ammonia oxidation reaction. Furthermore the $DeNO_x$ activity of the same catalyst was found to be less sensitive to the NO_2/NO_x feed ratio when compared to the iron zeolite: in particular, the copper zeolite exhibited a much greater steady-state $DeNO_x$ activity with NO_2/NO_x feed ratios below the optimal value of 0.5. The strong inhibiting effect of ammonia on the Standard SCR reaction at low temperatures previously reported for the Fe-zeolite catalyst was not observed over the copper zeolite system, which reacted differently to step changes of the ammonia feed concentration. Finally, formation of small amounts of nitrous oxide was detected over the copper catalyst even with negligible NO_2 feed contents, whereas N_2O formation occurred over the iron-based catalyst only when an excess of NO_2 was present in the gas feed mixture.

Acknowledgements

The financial support of Daimler AG is gratefully acknowledged. The Authors thank Dr. Bernd Krutzsch, Dr. Michel Weibel and Dr. Volker Schmeisser for useful discussions.

References

[1] P. Forzatti, L. Lietti, E. Tronconi, I.T. Horvath (Eds.), Nitrogen Oxides Removal—Industrial. Encyclopedia of Catalysis, first ed., Wiley, New York, 2002, , and references therein.
[2] T.V. Johnson, SAE Technical paper, 2009-01-0121.
[3] A. Grossale, I. Nova, E. Tronconi, Catal. Today 136 (2008) 18.
[4] H. Sjövall, L. Olsson, E. Fridell, R.J. Blint, Appl. Catal. B 64 (2006) 180.
[5] G. Madia, M. Koebel, M. Elsener, A. Wokaun, Ind. Eng. Chem. Res. 41 (2002) 3512.
[6] M. Devadas, O. Kröcher, M. Elsener, A. Wokaun, N. Soger, M. Pfeifer, Y. Demel, L. Mussmann, Appl. Catal. B 67 (2006) 187.
[7] E. Tronconi, I. Nova, C. Ciardelli, D. Chatterjee, M. Weibel, J. Catal. 245 (2007) 1.
[8] C. Ciardelli, I. Nova, E. Tronconi, D. Chatterjee, B. Bandl-Konrad, M. Weibel, B. Krutzsch, Appl. Catal. B 70 (2007) 80.
[9] I. Nova, C. Ciardelli, E. Tronconi, D. Chatterjee, B. Bandl-Konrad, Catal. Today 114 (2006) 3.
[10] D. Chatterjee, T. Burkhardt, B. Bandl-Konrad, T. Braun, E. Tronconi, I. Nova, C. Ciardelli, SAE Technical paper 2005-01-0965.
[11] G. Delbono, A. Fusari, A. Ubaldi, Il Vanadio: aspetti chimici e tossicologici, Ann. Fac. Medic. Vet di Parma, vol. XXIII, 2003, pp. 149–162.
[12] R.Q. Long, R.T. Yang, J. Catal. 207 (2002) 224.
[13] J.A. Sullivan, J. Cunningham, M.A. Morris, K. Keneavey, Appl. Catal. B 7 (1995) 137.
[14] S. Kieger, G. Delahay, B. Coq, B. Neveu, J. Catal. 183 (1999) 267.
[15] B. Ramachandran, R.G. Herman, S. Choi, H.G. Stenger, C.E. Lyman, J.W. Sale, Catal. Today 55 (2000) 281.
[16] W. Arous, H. Tounsi, S. Djemel, A. Ghorbel, G. Delahay, Catal. Commun. 6 (2005) 281.
[17] G. Delahay, S. Kieger, N. Tanchoux, P. Trens, B. Coq, Appl. Catal. B 52 (2004) 251.
[18] J.H. Baik, S.D. Yim, I.-S. Nam, Y.S. Mok, J.-H. Lee, B.K. Cho, S.H. Oh, Ind. Eng. Chem. Res. 45 (2006) 5258.
[19] J.H. Park, H.J. Park, J.H. Baik, I.S. Nam, C.H. Shin, J.H. Lee, B.K. Cho, S.H. Oh, J. Catal. 240 (2006) 47.
[20] B. Moden, J.M. Donohue, W.E. Cormier, H.-X. Li, Stud. Surf. Sci. Catal. 174 (2008) 121.
[21] B.J. Adelman, T. Beutel, G.-D. Lei, W.M.H. Sachtler, Appl. Catal. B 11 (1996) L1.
[22] L.T. Tsikoza, E.V. Matus, Z.R. Ismagilov, V.A. Sazonov, V.V. Kuznetsov, Kinet. Catal. 46 (2005) 281.
[23] A. Sultana, T. Nanba, M. Haneda, H. Hamada, Catal. Commun. 10 (2009) 1859.
[24] G. Qi, Y. Wang, R.T. Yang, Catal. Lett. 121 (2007) 111.
[25] L. Xu, R. McCabe, W. Ruona, G. Cavataio, SAE Technical paper 2009-01-285.
[26] J. Girard, G. Cavataio, R. Snow, C. Lambert, SAE Technical paper 2008-01-1185.
[27] A. Grossale, I. Nova, E. Tronconi, J. Catal. 265 (2009) 141.
[28] C. Ciardelli, I. Nova, E. Tronconi, B. Konrad, D. Chatterjee, K. Ecke, M. Weibel, Chem. Eng. Sci. 59 (2004) 5301.
[29] C. Ciardelli, I. Nova, E. Tronconi, M. Ascherfeld, W. Fabinski, Top. Catal. 42/43 (2007) 161.
[30] A. Grossale, I. Nova, E. Tronconi, D. Chatterjee, M. Weibel, J. Catal. 256 (2008) 312.
[31] I. Nova, C. Ciardelli, E. Tronconi, D. Chatterjee, B. Bandl-Konrad, AIChE J. 52 (2006) 3222.
[32] G. Delahay, D. Valade, A. Guzmàn-Vargas, B. Coq, Appl. Catal. B 55 (2005) 149.
[33] S. Brandenberger, O. Kroecher, A. Tissler, R. Althoff, Catal. Rev.: Sci. Eng. 50 (2008) 492, and references therein contained.
[34] M.S. Kumar, M. Schwidder, W. Grünert, U. Bentrup, A. Brückner, J. Catal. 239 (2006) 173.
[35] G. Li, C.A. Jones, V.H. Grassian, S.C. Larsen, J. Catal. 234 (2004) 401.
[36] M. Devadas, O. Kröcher, M. Elsener, A. Wokaun, G. Mitrikas, N. Söger, M. Pfeifer, Y. Demel, L. Mussmann, Catal. Today 119 (2007) 137.
[37] Q. Sun, Z. Gao, B. Wen, W.H. Sachtler, Catal. Lett. 78 (2002) 1.
[38] V. Sanchez-Escribano, T. Monatanari, G. Busca, Appl. Catal. B 58 (2005) 19.
[39] Y.H. Yeom, J. Henao, M.J. Li, W.M.H. Sachtler, E. Weitz, J. Catal. 231 (2005) 181.
[40] O. Krocher, M. Devadas, M. Elsener, A. Wokaun, N. Soger, M. Pfeifer, Y. Demel, L. Mussmann, Appl. Catal. B 66 (2006) 208.
[41] M. Li, J. Henao, Y. Yeom, E. Weitz, W.M.H. Sachtler, Catal. Lett. 98 (2004) 5.
[42] M. Koebel, G. Madia, M. Elsener, Catal. Today 73 (2002) 239.
[43] K. Rahkamaa-Tolonen, T. Maunula, M. Lomma, M. Huuhtanen, R.L. Keiski, Catal. Today 100 (2005) 217.
[44] D. Chatterjee, T. Burkhardt, M. Weibel, I. Nova, A. Grossale, E. Tronconi, SAE Technical paper 2007-01-1136.
[45] M. Wallin, C.J. Karlsson, M. Skoglundh, A. Palmqvist, J. Catal. 218 (2003) 354.
[46] H. Sjövall, R.J. Blint, A. Gopinath, L. Olsson, Ind. Eng. Chem. Res. 49 (2010) 39.